

M.Danilov, L.Laptin, I.Tichomirov, M.Titov, Yu.Zaitsev

**Aging tests of the proportional wire chambers
using $Ar/CF_4/CH_4(74:20:6)$, $Ar/CF_4/CH_4(67:30:3)$
and $Ar/CF_4/CO_2(65:30:5)$ mixtures
for the HERA-B Muon Detector**

Moscow 2000

The Muon Detector of the HERA-B experiment at DESY is a gaseous detector that provides muon identification in a high-rate hadronic environment. We present our studies on the properties of several fast gases, $Ar/CF_4/CH_4$ (74:20:6), $Ar/CF_4/CH_4$ (67:30:3) and $Ar/CF_4/CO_2$ (65:30:5), which have been found to fulfill muon detection requirements.

The severe radiation environment of the HERA-B experiment leads to the maximum charge deposit on a wire, within the muon detector, of 200 mC/cm per year. For operation in such an environment, the main criteria for the choice of gas turned out to be stability against aging. An overview of aging results from laboratory setups and experimental detectors for binary and ternary mixtures of Ar , CH_4 , CF_4 and CO_2 is presented and the relevance of the various aging results is discussed. Since it is not clear how to extrapolate aging results from small to large areas of irradiation, the lifetime of aluminum proportional chambers was studied under various conditions. In this paper we provide evidence that aging results depend not only upon the total collected charge. It was found that the aging rate for irradiation with Fe^{55} X-rays and 100 MeV α -particles may differ by more than two orders of magnitude.

1 Introduction.

The HERA-B experiment is a hadronic B-factory at DESY, operating presently under LHC-like conditions, five years before startup of LHC. The muon detection system in HERA-B is made up of three different types of gas proportional chambers: tube, pad and pixel [1, 2]. The readout of the chambers is based on the ASD-8 amplifier shaper discriminator chip developed by the University of Pennsylvania [3]. Strong restrictions on the gas choice are imposed by the harsh operating conditions. In addition to the high radiation load, resulting in an accumulated charge on a wire of up to 200 mC/cm per year, the muon chambers have to withstand the presence of heavily ionizing particles, neutrons, and low energy gammas. The first level trigger requires high hit efficiency and fast signal collection within the 96 ns time interval between two consecutive bunch crossings.

In section 2, the requirements and limitations of the choice of gases for the muon system are explained and the chamber characteristics studied with several fast Ar/CF_4 -based mixtures are discussed. The overview of aging results from laboratory setups and experimental detectors for binary and ternary mixtures of Ar , CH_4 , CO_2 and CF_4 is presented in section 3. Since it is not clear how to extrapolate aging results from laboratory setups, when irradiating a small region of the wire, to large areas of irradiation with hadronic particles, we have studied aging properties of aluminum proportional chambers operated with $Ar/CF_4/CH_4$ and $Ar/CF_4/CO_2$ mixtures with Fe^{55} and Ru^{106} sources and in 100 MeV α -beam. The results of these aging tests performed in a variety of conditions are summarized in sections 4 and 5.

2 Selection of fast gas mixtures.

Large area gaseous detectors operated under high intensity particle fluxes impose new requirements for gas selection. The HERA-B muon system, with a total gas volume of $8\ m^3$, puts rather stringent constraints on the gaseous medium to be used: extremely low aging, high sparkproofness, good electrical properties (high drift velocity v_d , convenient operating electric field E/p), good chemical properties (non-flammable, non-poisonous). Since it is necessary to replenish part of the gas to avoid contamination by air, the cost of the component gases is also an important issue for gas selection.

For a minimum working voltage, noble gases are usually chosen since they require the lowest electric field intensities for avalanche formation. However,

photons limit the attainable gas amplification in the *Ar*-operated counters to $\sim 10^4$ without encountering a permanent discharge induced by the photon-feedback mechanism taking place at the cathode. This problem can be remedied by the addition of gases, such as hydrocarbons, alcohols, CO_2 , H_2O , NH_3 . These molecular additives act like quenchers and improve the operational stability of the counter by absorption of ultraviolet photons from the multiplication process, de-excitation of *Ar* atoms [4], and by the charge transfer mechanism prevent the neutralization of argon ions at the cathode, thus reducing electron emission through predissociation of quench gas ions [5, 6]. Some of the polyatomic gases will also effectively increase the total ionization by the Penning effect.

Moreover, in pure *Ar* the electron drift velocity is ~ 30 times lower than in CH_4 , although their elastic cross sections are nearly identical. However, the addition of even small quantities ($\sim 0.1\%$) of a molecular gas increases the drift velocity in argon threefold and also alters the shape dependence of v_d on E/P [7, 8]. In general, the drift velocity v_d varies inversely with the product of the total scattering cross-section σ_{sc} and the square root of the mean electron energy $\bar{\epsilon}$ [9, 10]. Traditionally, the fast gas mixtures were achieved by adding to *Ar* a polyatomic gas (usually a hydrocarbon or CO_2) which effectively shifts the low energy part of the electron distribution function into the region of the Ramsauer-Townsend (R-T) minimum, located at ~ 0.5 eV, of the momentum transfer and total electron scattering cross-section of *Ar*. The cooling of the electron swarm occurs as the energetic electrons quickly transfer their energy to rotational and vibrational modes of the polyatomic gas, whose scattering cross-section has a large inelastic component to the right of the R-T minimum. Furthermore, the cooling effect of a given gas in a high electric field gas amplification region need not be the same as its cooling effect in the lower electric field drift region. As was shown in [11], the very similar effects observed in the *Ar/CH₄* and *Ar/CO₂* mixtures in the avalanche region are contrasted with different properties of these gases in the lower electric fields: CO_2 is a much cooler gas than CH_4 in the drift region, as is evidenced by the measured diffusion coefficients [12]. These results open the possibility of choosing a gas mixture to separately optimize the desired drift and gain behavior in a particular application.

Almost twenty years ago, CF_4 has been proposed for high rate environments as a most effective additive to raise the drift velocity in noble gases. This gas obtains its large drift velocity because of the sizeable Ramsauer-

Townsend dip in the elastic cross-section which coincides with a very large vibrational inelastic cross-section [13]. For the $Ar/CF_4(90:10)$ mixture the electron drift velocity was found to exceed $10 \text{ cm}/\mu\text{s}$, which is twice as fast as for the conventional mixture $Ar/CH_4(90:10)$ [9]. Further increase of the CF_4 fraction in Ar/CF_4 mixtures tends to push the maximum drift velocity to the higher field region, but when the percentage of CF_4 becomes larger than 20 %, the v_d is the same whatever the mixture, indicating that it's mainly controlled by the CF_4 cross section [14, 15, 16]. The lower vibrational modes, as well as the lower-lying negative ion states of CF_4 as compared to CH_4 , may account for the superior drift properties of the Ar/CF_4 mixtures compared to Ar/CH_4 [17, 18].

However, all binary Ar/CF_4 mixtures have rather poor energy resolution, compared to Ar/CH_4 , due to the production of negative ions [9, 19]. The dissociative attachment processes in CF_4 are the only mechanisms leading to negative ion (F^- , CF_3^-) formation, via two broad and overlapping resonances located between 4.5 and 10 eV [14, 20], and can cause serious inefficiencies in the collection of electrons and degrade the position resolution. The main evidence for the electron attachment is the direct measurement of the effective ionization coefficient $\bar{\alpha} = \alpha - \eta$; where α and η are, respectively, the electron impact ionization and electron attachment coefficients. The negative values of $\bar{\alpha}$ were observed in the drift region in pure CF_4 , $Ar/CF_4(80:20)$ and $Ar/CF_4/H_2O(80:18:2)$ mixtures. Very interestingly, the electron thermalizing properties effected by substituting 10 % of CF_4 in the $Ar/CF_4(80:20)$ by 10 % of CO_2 virtually eliminates the electron attachment in $Ar/CF_4/CO_2(80:10:10)$ mixture [17].

Moreover, due to the small CF_4 quenching cross-sections of metastable Ar -states [21, 22], the Ar/CF_4 mixtures are not sufficiently self-quenching and show an intolerable level of afterpulsing even at moderate gas amplifications (see also section 2.1). This is not the case for the Ar /hydrocarbon mixtures, where no significant afterpulsing was observed so far at moderate gas gains. At the same time, some of the Ar/CO_2 mixtures are known to suffer from a low sparkproofness [23], since the quenching ability of CO_2 is smaller than that of hydrocarbons.

The advantage of the enhanced drift velocity of CF_4 could be realized either in binary CF_4 /quencher or in ternary Ar/CF_4 /quencher mixtures. The choice of CH_4 among the hydrocarbons is dictated by the requirements that the drift velocity in the lighter hydrocarbons is larger than that in the heav-

ier ones [15], especially in the low-field region. Fig. 1 shows the drift velocity for the $Ar/CF_4/CH_4(74:20:6)$, $CF_4/CH_4(90:10)$, $Ar/CF_4/CO_2(65:30:5)$, $Ar/CF_4/CO_2(80:10:10)$ and $CF_4/CO_2(90:10)$ mixtures, as a function of the electric field strength at atmospheric pressure. These results are taken from Refs. [17, 24, 25, 26]. As can be seen from the curves, the CF_4/CH_4 mixtures are significantly faster than CF_4/CO_2 for any given value of E/P . The use of $Ar/CF_4/CH_4$ could be more preferable for high-rate proportional chamber applications than CF_4/CH_4 mixtures, since the former shows fast rises in the drift velocity for the relatively low fields, with respect to the latter, and the mobilities of CH_4^+ ions in Ar are much higher than those in CF_4 , which is desirable in terms of space charge effects [15, 26]. An additional disadvantage of the CF_4/CH_4 mixture is the necessity to operate at high electric fields E/P for a sufficient gas gain, resulting in exceedingly high voltages in the chamber. This could introduce a problem of electrostatic instability of anode wires in large chambers. Furthermore, considerations of cost and safety led us to consider $Ar/CF_4/CH_4$ mixtures as a reasonable compromise between many experimental requirements. An optimization of the exact proportions of Ar , CF_4 , and CH_4 in the mixture was performed using the Magboltz and Garfield simulation programs. As a result of simulation, $Ar/CF_4/CH_4$ (74:20:6) and another mixture with a reduced CH_4 content $Ar/CF_4/CH_4$ (67:30:3) were chosen for muon detector operation. Unfortunately, mixtures with hydrocarbons have a tendency to cause polymerization effects, while CO_2 quencher has been proven to give a much longer lifetimes. However, addition of CO_2 appreciably changes the drift properties of the $Ar/CF_4/CO_2$ mixture, compared to the case of $Ar/CF_4/CH_4$; reduces the maximum drift velocity, and shifts it to the higher field region. In practice, we chose $Ar/CF_4/CO_2(65:30:5)$ mixture, as a fall back gas, if the aging criterion becomes dominant.

Finally, in the $Ar/CF_4/CH_4$ (74:20:6), $Ar/CF_4/CH_4$ (67:30:3) and $Ar/CF_4/CO_2$ (65:30:5) mixtures, electron attachment processes may complicate gas performance. However, the primary ionization in the chamber cell is large enough and more than compensates for any losses due to electron attachment, especially since only hit information is processed in the muon detector.

2.1 Tube Chamber Characteristics.

In this paper, we address the problem of gas selection and present the measured data only for tube chambers. The tube chamber is a closed-cell proportional wire chamber made from an aluminum profile (wall thickness 2 mm)

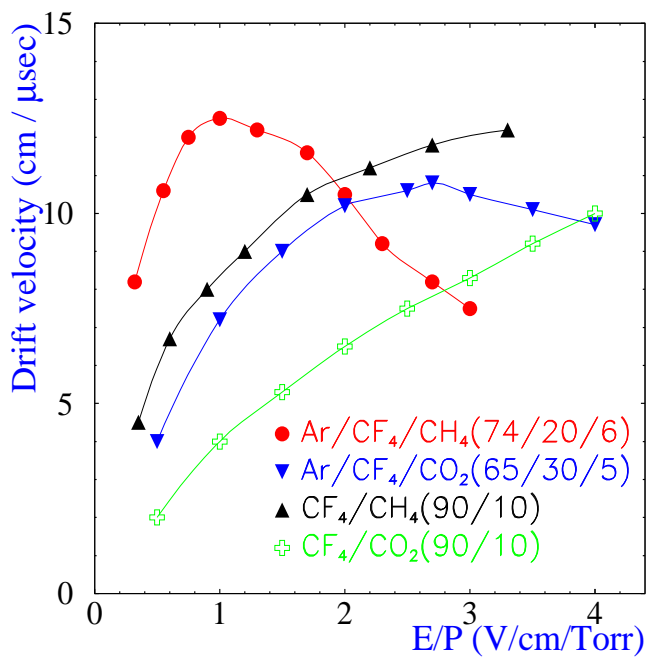


Figure 1: Electron drift velocity as a function of E/P

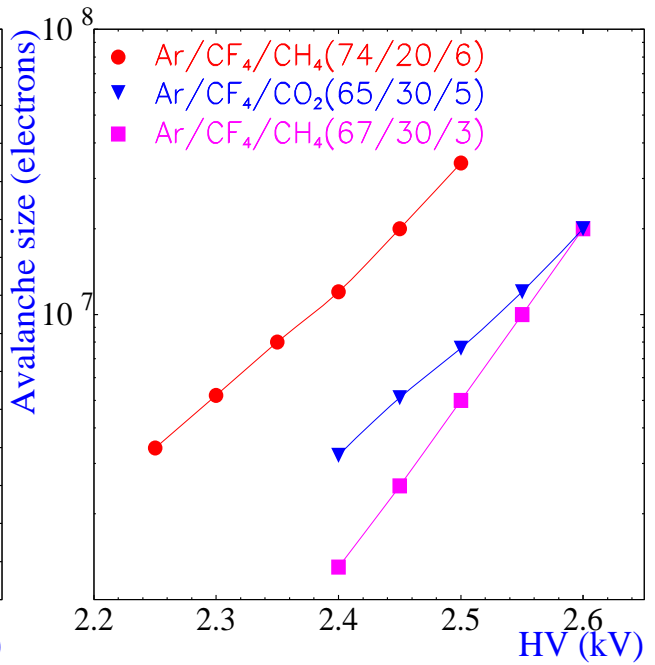


Figure 2: Avalanche size curves as a function of HV for 5.9 keV X -rays

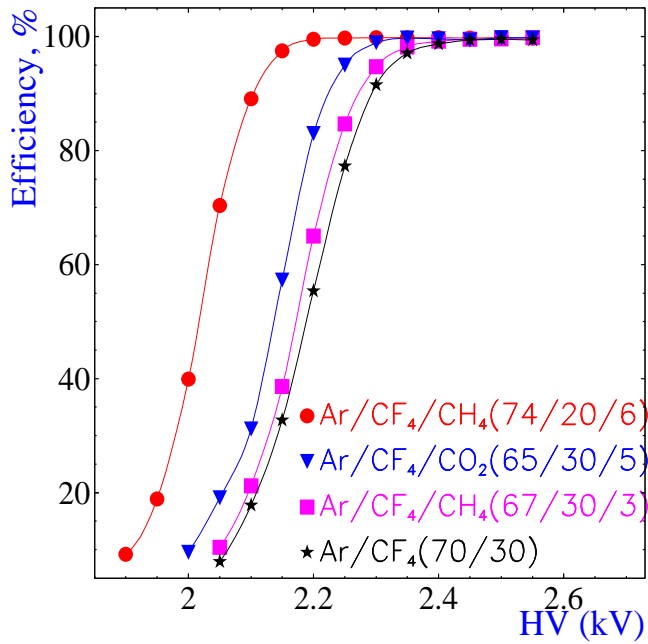


Figure 3: Tube chamber efficiency as a function of HV

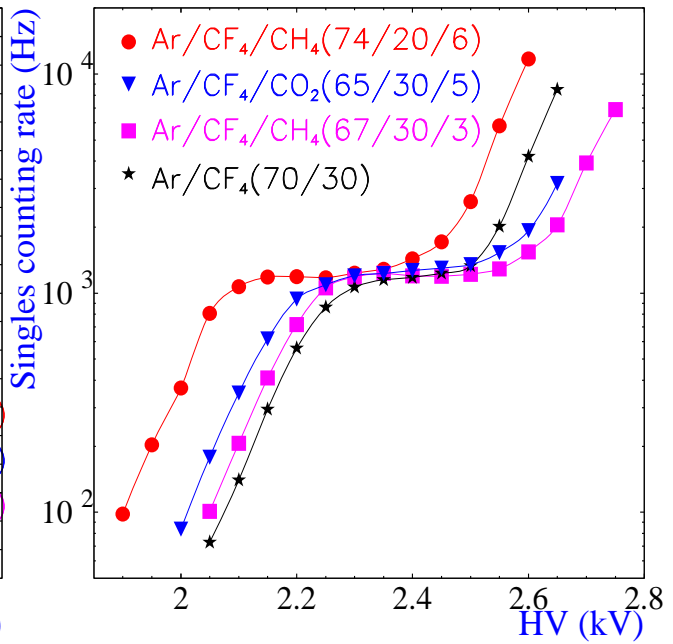


Figure 4: Singles counting rates for a tube chambercell as a function of HV

with a drift cell $14 \times 12 \text{ mm}^2$ in cross section. Fig. 5 shows the schematic drawing of the tube chamber. A gold-plated tungsten wire of $45 \mu\text{m}$ diameter and a length of nearly 3 m is stretched inside each cell and fixed mechanically with pins at the end of the chamber. In order to prevent efficiency losses due to dead spaces between cells, the tube chamber consists of two layers, each having 16 drift cells, shifted with respect to each other by half a cell size.

Figure 5: Schematic drawing of the tube chamber. Dimensions are indicated in units of mm.

Firstly, we have collected the Fe^{55} spectra for each mixture under study: $Ar/CF_4/CH_4$ (74:20:6), $Ar/CF_4/CH_4$ (67:30:3) and $Ar/CF_4/CO_2$ (65:30:5) with a goal of inferring the response to minimum ionizing particles. Measured pulse heights were converted to avalanche sizes, which correspond to the total number of electrons in the avalanche. The gas gain value can be obtained by dividing the observed pulse size by ~ 200 , the average number of primary electrons, if the mixture has no electron attachment. Fig. 2 shows the total avalanche size increasing in an exponential manner with the high voltage, within the limits of the proportional region. It has been shown previously [27] that the onset of secondary gas effects such as space charge saturation may be detected as a break in the expected scaling of the gas gain with respect both to anode surface field and to gradient of the electric field near the wire. It should be noted that for these data taken with an Fe^{55} source with its fixed initial charge (~ 200 electrons), a particular value of gas gain is equivalent to a definite value of the total charge in the avalanche. Space charge effects depend on the total avalanche size and distribution of the positive ion cloud. Hence, these numerical results cannot be automatically applied to other ionization sources with different magnitudes or distributions of the initial charge.

Secondly, the tube chamber characteristics have been studied on the 3 GeV electron test beam at DESY. The beam intensity was $\sim 1 \text{ kHz/cm}^2$. The trigger was initiated by a coincidence of four beam-defining scintillator counters, between which the chamber was positioned. Then, the number of events with at least one hit in the double layer chamber, within the 96 ns, ver-

sus the number of triggered events yields an efficiency. Fig. 3 shows the measured efficiency for the mixtures being studied, as a function of high voltage. This figure demonstrates, that the actual efficiency is approximately 100 % for the double layer chamber. However, for a single layer the usage of $Ar/CF_4/CO_2(65:30:5)$ mixture results in about 7 % of signals registered outside the 96 ns (for perpendicular tracks), while in $Ar/CF_4/CH_4$ mixture nearly all signals are collected within the 96 ns. Fig. 4 presents singles (untriggered) counting rates for a tube chamber cell as a function of high voltage. From these curves, wide high voltage plateaus for a stable and efficient operation with the $Ar/CF_4/CH_4(74:20:6)$, $Ar/CF_4/CH_4(67:30:3)$ and $Ar/CF_4/CO_2(65:30:5)$ gases are observed, where the counting rate is roughly uniform. Real afterpulses and multiple hits of ASD-8 per signal both contribute to the rise in singles rate curves, above the nominal beam intensity, with increasing high voltage. In comparison, $Ar/CF_4(70:30)$ mixture will not guarantee stable and efficient operation over sufficient high-voltage range in the tube chambers. The difference in singles rate curves, and correspondingly in detection efficiency, between $Ar/CF_4(70:30)$ and $Ar/CF_4/CH_4(67:30:3)$ may be attributed to the enhanced gas electron production efficiency and smaller electron attachment for the latter mixture. In addition, onset of secondary avalanches in Ar/CF_4 limit the maximum operating voltage to 2.5 kV (see Fig. 4), thus causing a drastic decrease in the counting rate plateau width.

The results presented here justify the choice of $Ar/CF_4/CH_4$ (74:20:6), $Ar/CF_4/CH_4$ (67:30:3) and $Ar/CF_4/CO_2$ (65:30:5) gases for muon detection with high efficiency.

3 General characteristics of aging processes.

Aging effects in proportional wire chambers, a permanent degradation of operating characteristics under sustained irradiation, has been and remains the main limitation to their use in high-rate experiments [28]. Many processes are expected to occur simultaneously in the gaseous discharges surrounding the wire and it is nearly impossible to obtain a quantitative chemical description in each particular case. There is much experimental information, excellently summarized in [29, 30, 31, 32], that suggests the wire chambers lifetime could be affected, and in some cases dramatically, by the nature and purity of the gas mixture, materials used in contact with the gas, by different additives,

and trace contaminants.

While the specific reactions responsible for wire chamber aging are extremely complex, a qualitative description of the aging phenomena in different gases could be obtained from similarities between chemical processes in wire chamber avalanches and those that occur in the better-understood low-pressure rf-plasmas [30, 31, 33, 34, 35]. During wire avalanches many molecules break up by collisions with electrons, de-excitation of atoms, and UV-photon absorption processes. Whereas most ionization processes require electron energies greater than 10 eV, the breaking of the chemical bonds in molecules and formation of free radicals requires only 3-4 eV, and could lead to a large abundance of free radicals over the ions in the wire avalanches. Similar to plasma polymerization [36], a free-radical polymerization seems to be the most appropriate mechanism of the wire chamber aging. Since free radicals are chemically very active they will either recombine back to original molecules or other volatile species, or form new cross-linked molecular structures, which could react further to produce chain-like polymers of increasing molecular weight, thus lowering the volatility of the resulting product. When the growing of polymerized chain becomes large enough for condensation to occur, it will diffuse to the electrode surface. The polymer deposition mechanism can be conceived as a phenomenon that occurs whenever the gaseous species fails to bounce back on collision with a electrode surface, including a surface of particles already formed in the gas discharges. Initially the polymer could be held to the surface very weakly, unless some additional chemical reaction takes place between the polymer atoms and atoms of the wire material. Furthermore, many free radicals are expected to have permanent or induced dipole moments; therefore, electrostatic attraction to a wire could play a significant role in the polymer deposition process. Thus, aging effects in gaseous detectors would lead to deposition of thin, very high quality polymers on the anode wires, and would result in a loss of the gas gain and degradation of ionization measurements. Deposits on cathodes can induce discharges by secondary electron emission (or Malter effect [37]), and would lead to chamber breakdown.

Traditionally, the aging rate was parameterized as a normalized gas gain loss [30]:

$$R = -\frac{1}{G} \frac{dG}{dQ} (\% \text{ per } C/cm)$$

where G is an initial gas gain, dG is the loss of gas gain after collected

charge Q per unit length. The parameterization used above implicitly assumes that the gain drop depends linearly on the charge collected per unit length of the wire, and that the aging rate is only a function of the total collected charge, independent of gas gain and radiation intensity. In reality, this assumption is not fulfilled. Several examples in the literature [38, 39, 40, 41, 32] clearly indicate that the degree of aging for a given radiation dose could also depend upon the mode of operation, being larger for smaller current densities, other conditions being held constant. These observations raise a question on the relevance of aging results, obtained in accelerated aging tests with extremely high current densities, extrapolated to normal conditions. Moreover, aging studies of ATLAS muon drift tubes, have shown a strong dependence of the aging rate on the mode of operation (irradiation rate, high voltage) and size of the irradiated area [42]. Furthermore, it has been found that the aging rate in the HERA-B honeycomb tracker chambers varies substantially, when changing from γ irradiation to heavy ionizing particles (see section 3.1). This paper presents evidence that the aging rate for irradiation with 5.9 keV X -rays and 100 MeV α 's may differ by more than two orders of magnitude (see sections 4 and 5). Furthermore, it was recently reported in [43] and it will be shown in a subsequent paper [44], that the rate of polymer deposition could also be affected by the mode of operation, size of the irradiated area and water addition.

These results exclude the possibility to extrapolate aging rates obtained in the laboratory setups by irradiating a small region of the wire to the large areas of irradiation in hadronic environment. Therefore, for each particular case, the final decision for long-term stability of operation should be taken only after obtaining similar performance in conditions as close as possible to real ones.

3.1 Results from wire chambers operation.

Over the last few decades, an impressive variety of experimental data has been accumulated and it is not feasible to go through all published results. In addition, new results make doubtful the quantitative comparison of aging properties, realized at very different conditions. Therefore, we will present below only a brief summary of the most recent data, focusing on the binary and ternary mixtures, containing Ar , CH_4 , CO_2 and CF_4 .

There are a lot of reports that clearly indicate premature aging in Ar/CH_4 filled wire chambers exposed to intense radiation [38, 45, 46, 47, 48]. The

polymerization of CH_4 is attributed to the hydrogen deficiency of radicals and their ability to make bonds with hydrocarbon molecules [30, 36], leading to the buildup of deposits on the anode wires, which usually contain carbon and lighter elements.

Attempts were made to replace the organic quenchers with more stable ones, such as CO_2 . However, the gradual decomposition of CO_2 in Ar/CO_2 mixtures also takes place and stable operation was found to be possible up to charges of 0.5-0.7 $\frac{C}{cm \text{ wire}}$ [31, 49]. Furthermore, carbon dioxide is also known for its carbon buildup, which occurs specifically at the cathode [6], however, this carbon layer did not affect the performance of the drift tubes [49]. Another effect, which is enhanced in Ar/CO_2 mixtures compared to gases containing hydrocarbon quenchers, is the spurious counting rate (noise), that presumably comes from the spikes on the wires. This noise can be cured by the addition of water vapor to the drift gas [49].

The aging studies in the ternary mixtures $Ar/CH_4/CO_2$ indicate the dependence of the aging rate on the particular set of operating conditions, in some cases being smaller for larger CH_4 content in the mixture [39, 50, 51]. The stable operation far beyond 0.6 $\frac{C}{cm \text{ wire}}$ was observed for $Ar/CH_4/N_2/CO_2$ (94:3:2:1) + 1200 ppm of H_2O mixture, however, some conditions where found were only a tenth of nominal lifetime was achieved [47]. Moreover, for the $Ar/CH_4/N_2/CO_2$ mixture, measurements have shown that their sensitivity to aging decreases with decreasing CH_4 and increasing CO_2 content.

The use of gases having CF_4 as a component was found to be attractive in the plasma processes, since the CF_4 is an ideal source for a variety of reactive neutral and ionic fragment atoms and molecules, and especially neutral fluor, which is a desirable active species in etching processes [52]. The CF_4 molecule is relatively inert in its electronic ground state, but all excited electronic states of CF_4 and CF_4^+ ion lead to dissociation. Below the onset of electronic excitations, which is rather high - 12.5 eV, collisions of electrons with CF_4 molecule lead to elastic scattering, vibrational excitation and dissociative attachment. Above this energy, dissociation of the CF_4 into neutrals or charged fragments becomes significant [14, 20]. Actually, in plasma environment CF_4 -based gases are used for both etching and deposition processes, the distinction being made by the gas and its amount with which CF_4 is mixed. The balance between these processes is called 'competitive ablation and polymerization'. In general, the addition of oxygenated species shifts the chemistry of CF_4 plasmas toward etching, while the addition of hydrogenated

species shifts the chemistry toward polymerization [34, 36, 53, 54]. For example, the polymer formation by CF_4 plasmas in the presence of CH_4 was observed [36].

In the wire chamber operation, the usage of CF_4 is also quite controversial. Many studies have demonstrated excellent aging properties, up to $10 \frac{C}{cm \text{ wire}}$, of CF_4/iC_4H_{10} (80:20) avalanches [55, 56], which also has an ability to etch both silicon-based [30, 56] and hydrocarbon [56] deposits from the previously aged gold-plated wires. However, another proportions of CF_4 and isobutane could totally change the chemical reactions on the surface of the anode wire. Heavy carbonaceous deposits were formed on the gold-plated wires irradiated in the mixtures CF_4/iC_4H_{10} (95:5) and CF_4/iC_4H_{10} (20:80). The absence of fluorocarbon deposits on the anode wires indicates that the deposits were formed only from iC_4H_{10} , without incorporation of CF_x fragments. Details of the chemical model and aging results in the CF_4/iC_4H_{10} are presented elsewhere [34]. Another gas observed to form heavy carbonaceous anode deposits was CF_4/C_2H_4 (95:5) [34]. At the same time, the 4 % addition of CF_4 has been shown to inhibit anode damage in Ar/C_2H_6 (50:50) mixture up to the doses of $1.5 \frac{C}{cm \text{ wire}}$ [40]. Aging studies have been also performed with the CF_4/CH_4 (90:10) gas mixture and no deterioration was found up to 1.9 C/cm of the wire [57]. Finally, it should be noted, that most of the aging studies in the CF_4 /hydrocarbon mixtures, were performed by irradiating a small region of the wire under well controlled laboratory conditions. At the same time, several painful experiences with aging are known from the high energy experiments. The D0 muon drift chambers, filled with $Ar/CF_4/CH_4$ (80:10:10) undergo a fast aging when operated in a radiation environment. Vapors from a glue used in the construction were deposited on the wires in a sheath, with the deposition rate proportional to accumulated charge [58]. Furthermore, operation in the high-rate hadronic HERA-B environment showed that the aging rate could depend on the type of ionization and size of the irradiated area [59, 60]. The severe anode and cathode aging effects were observed in the honeycomb chambers tested in the HERA-B conditions with CF_4/CH_4 (80:20) and $Ar/CF_4/CH_4$ (74:20:6) mixtures after the radiation dose of several mC per cm of the wire. This effect was surprising since the chambers were proved to be immune a very large X -ray doses, up to the 5 C/cm of the wire.

The aging properties of the gas mixtures $Ar(Xe)/CF_4/CO_2$, which by analogy with plasma experiments should provide etching environments in the wire avalanches, have been also widely investigated over the past years. The

radiation tests of the ATLAS straw tubes using $Xe/CF_4/CO_2$ mixture showed no signs of aging for a integrated charge of up to 8 C/cm [61, 62]. However, the detailed examination of anode wires and straw walls (cathode) after irradiation had shown evidence for the etching processes on both surfaces [63]. Another interesting phenomena was found in straw tubes irradiated under exceedingly high current densities in $Xe/CF_4/CO_2$ mixture. After an accumulated charge of 9 C/cm the ‘anode swelling effect’ was observed, where destruction of gold coating of the gold-plated tungsten wires, followed by the tungsten oxidation [64, 65]. Recently, it was also reported [59, 60], that under a high radiation intensity in $Ar/CF_4/CO_2$ (65:30:5) mixture, gold-plating of tungsten wires can be etched away completely exposing the tungsten. However, the addition of water to the $Ar/CF_4/CO_2$ (65:30:5) was found to reduce the rate of etching processes, and the honeycomb chambers were able to survive radiation doses of up to $2 \frac{\text{C}}{\text{cm wire}}$. The chemical etching processes in the $Ar/CF_4/CO_2$ are likely to be responsible for the enhanced removal of the diamond coating observed in MSGC-GEM chambers [66].

Amazingly, extremely rapid aging has been observed for pure CF_4 and in $Ar/CF_4/O_2$ (50:40:10) mixture, which were expected to have strong etching abilities [34, 67]. In the former case, the aging process was related to chemical processes at the cathode, where trace fluorocarbon deposits were found. This type of aging phenomena was found to be cathode-material-dependent, and resulted in a loss of gas gain rather than in a self-sustained discharge. For the latter case, although C , O , and F elements were observed on the anode wire, it is likely that the rapid aging was as a result of the same (cathode phenomenon) observed in pure CF_4 . The fluorination of the anode wires, found after exposure in $Ar/CF_4/O_2$ (50:40:10) avalanches, can cause anode aging in addition to cathode effects [34]. A further phenomena due to the consistency of the cathode surfaces was observed in ATLAS aluminum drift tubes operated in $Ar/CF_4/N_2/CO_2$ (94.5:0.5:2:3). Here, no change in gas gain for the tubes was found up to an accumulated charge of $5 \frac{\text{C}}{\text{cm wire}}$. However, the increased count rate at the beginning of the tests, due to afterpulses in this gas at high gains decreased with the time to the level, when no significant afterpulsing was observed. This reduction was suggested to be due to the increased layer of fluor and oxygen found at the cathode [42]. Similar effects were also found during the long-term irradiation of drift tubes with stainless steel cathodes in pure CF_4 [68].

These aging results clearly demonstrate that the presence of large amounts

of CF_4 in the mixture does not necessarily ensure good aging properties. Moreover, perfluorocarbons represent the most extreme case of ablation competing with polymer formation. Therefore, all attempts to improve the aging performance of the mixtures by adding CF_4 must be tested in the actual environment.

An abundance of literature exists describing the effect of certain additives with oxygen-containing groups, like water, alcohol, methylal, oxygen. These components, added to the mixture in small concentrations, usually (but not always) extend the chamber lifetime, especially against the polymerization of hydrocarbons. Of special interest is the addition of water vapors, that has been found to suppress effectively polymerization in wire chambers [47, 69], to prevent Malter breakdowns [70], or even to restore the original operation in aged counters [41, 71]; a few hundred to a few thousand *ppm* of water are generally used. The most natural mechanism by which water impedes Malter breakdowns and significantly improves the analog response of the aged counters comes from the fact that water tends to increase the conductivity of the damaged electrodes [30, 41]. In addition, water could effectively suppress the secondary photon-mediated phenomena, if the UV photons from carbon excitations are responsible for the photoionization at the cathode [72]. At the same time, the exact mechanism by which water stops or reduces the aging rate in wire chambers is not clearly understood. One possible explanation could be gained from the similarities with plasma chemistry, where water acts like a blocking agent of the chain growth mechanism, reacting with polymer precursors, thereby decreasing the concentration of free radicals available for polymerization [36]. Another explanation is that water, due to its large dipole moment, could effectively slow-down electrons in the avalanches making the mixture ‘cooler’. In this case, aging effects resulting from free radical polymerization would be reduced, since fewer radicals would be formed in the wire avalanches. Finally, it is well established, that aging effects in the wire chambers, even when they are entirely due to polymerization of gas mixture components can be accelerated by the discharges (glow discharges of sparks) and photoelectric feedback [72, 73]. These effects are strongly dependent on the quality and type of the electrodes: surfaces of anode wire or cathode could be rather imperfect, thus, ‘triggering’ polymerization in wire chambers. Known remedies for aging in this case are also water and alcohols, which may prolong the lifetime considerably. Furthermore, aging can be initiated by the trace contaminants such as *Si*, halogens (other than CF_4), sulfur, phthalats,

benzine rings, which are either initially present in the gas, or result from outgassing of solid materials in contact with gas. The detailed summary of the influence of commonly used materials on aging properties may be found in [30, 63]. When constructing large systems, one should before to certify the gas purity and chemical reactivity of various materials in order to avoid the presence of 'bad' molecules in contact with the active gas volume.

4 Aging results from laboratory tests.

We have carried out a laboratory study of the aging properties of $Ar/CF_4/CH_4$ (74:20:6) mixture, when exposed to an intensive Fe^{55} source, and of $Ar/CF_4/CH_4$ (67:30:3) and $Ar/CF_4/CO_2$ (65:30:5) mixtures, both irradiated with a Ru^{106} source, up to a total radiation dose of 2 C/cm of the wire. In each test, a single cell of the proportional tube chamber was irradiated through a hole in the cathode wall, closed with thin *Al* foil, in the center of the 50 cm long cell. The irradiated area was limited by a collimator to about 30 mm of the wire for the Fe^{55} source and to 10 mm for the Ru^{106} source. While the Fe^{55} 5.9 keV X-rays produce an ionization cluster in the chamber cell, corresponding to ~ 200 primary electrons, the Ru^{106} source provides 3.54 MeV electrons from the decay of Rh^{106} , which leaves an ionization track with ~ 90 primary electrons per cm. The degree of aging was determined quantitatively by comparing Fe^{55} spectra, measured at the irradiated and reference positions of the wire, using the same electronics chain. This method removed problems arising from the Fe^{55} peak position movement due to changes in the pressure, the temperature, and gas mixture itself. The total collected charge was determined by integrating continuously the recorded anode current. The gas flow rate was 1 liter/hour for all tests.

A standardized set of conditions was established for the Fe^{55} irradiation of the $Ar/CF_4/CH_4$ (74:20:6) mixture, corresponding to a current of $0.7 \mu A/cm$ at a HV=2.65 kV. For irradiation with the Ru^{106} source, the high voltages for operation in $Ar/CF_4/CH_4$ (67:30:3) ($Ar/CF_4/CO_2$ (65:30:5)) mixtures were set to 2690 V (2790 V), corresponding to current densities of $1.2 \mu A$ ($0.9 \mu A$). The different current densities for the irradiation of $Ar/CF_4/CH_4$ (67:30:3) and $Ar/CF_4/CO_2$ (65:30:5) mixtures is attributed to the reduced source strength for the latter case, due to the larger thickness of *Al* foil used as a cathode above the irradiated region of the wire. The high voltages used during the aging studies already exceed the proportional mode of gas

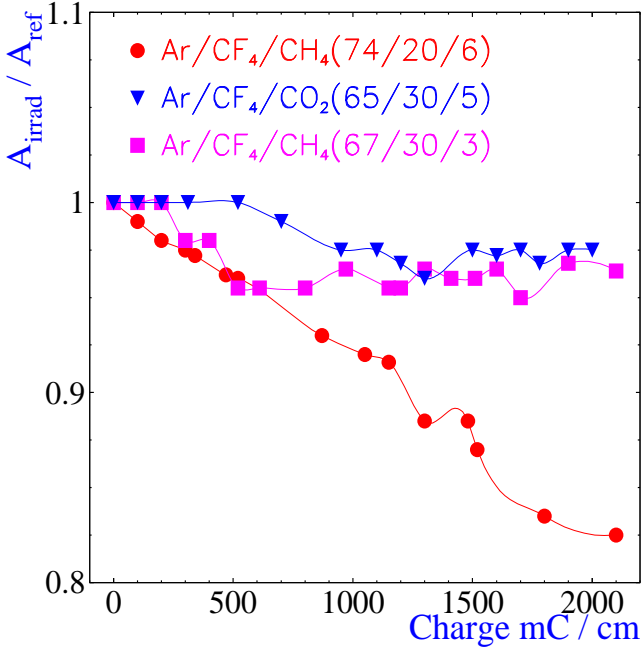


Figure 6: Ratio of Fe^{55} peak positions at irradiated and reference spots as a function of the accumulated charge.

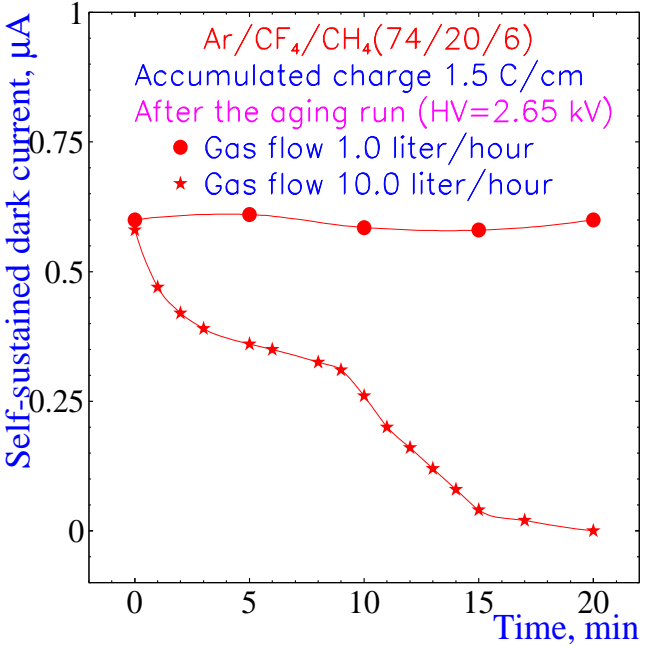


Figure 7: Measured dependence of a self-sustained dark current as a function of gas flow, after the removal of the irradiation source.

amplification, therefore, events with higher pulse heights than those in the proportional mode also appear at these voltages.

Fig. 6 shows the ratio of Fe^{55} peak positions, measured at irradiated and reference spots as a function of the accumulated charge. For the $Ar/CF_4/CH_4$ (74:20:6) mixture, the relative mean amplitude $\frac{A_{irrad}}{A_{reference}}$ monotonously dropped to about 85 % of the initial value, after the radiation dose of $2 C/cm$ of the wire, corresponding to $R \sim 8 \% / C/cm$. Such a rate of gas gain losses could be acceptable for the long-term operation of the muon chambers in HERA-B. However, after a collected charge $\sim 1 C/cm$ significant self-sustained dark current appeared in addition to those normally associated with radiation. This dark current persisted even after the removal of the radiation source, but it was totally quenched, either by a large increase in the gas flow rate, from 1 liter/hour to 10 liters/hour (see Fig. 7), or by turning off the high voltage. This phenomena is associated with the polymer coating and subsequent charge buildup on the cathode surface, by a mechanism similar to the well known Malter discharge [37].

Irradiation with the Ru^{106} source of $Ar/CF_4/CH_4$ (67:30:3) and $Ar/CF_4/CO_2$ (65:30:5) mixtures led to R values consistent with zero (see Fig. 6). Such promising aging behavior make these gases suitable candidates for use in the tube chambers. Unfortunately, as will be reported in section 5, the aging

results, obtained in the high-rate hadronic environment when irradiating a large area chamber differ significantly from those described above.

5 Aging studies in a 100 MeV α -beam

5.1 Aging in $Ar/CF_4/CH_4(74:20:6)$ gas mixture.

After the tests with radioactive sources, aging studies with the $Ar/CF_4/CH_4(74:20:6)$ mixture were carried out by irradiating a single layer tube chamber in a 100 MeV α -beam in Karlsruhe (see Fig. 8). Due to the small range of the 100 MeV α 's in aluminum, the thickness of the *Al*-wall was reduced to $\sim 200 \mu m$. The α -beam intensity was almost uniform over the beam area $8 \times 8 cm^2$. This allowed a constant irradiation of four wires fully, and, in addition, two wires were exposed over half of their cell width. All wires were equipped for analog readout. Furthermore, for one of wires, which we will call a 'reference wire', two holes were made in the chamber wall - within the region of irradiation and outside of it. Both holes were closed with kapton foil. For the 'reference wire', it was possible to measure the degree of aging by comparing the Fe^{55} spectra at the two positions of the same wire.

A premixed gas mixture of $Ar/CF_4/CH_4(74:20:6)$ was transported by stainless-steel tubes connected directly to the tube chamber inlet and outlet. The gas flow was in serial inside a chamber from one cell to another, with the flow rate about 6 liters/hour. The operating voltage was set to 2.35 kV, corresponding to a gas gain $\sim 4 \times 10^4$, measured with Fe^{55} X-rays. The radiation intensity varied during the aging studies by a factor of 3, thus excluding any possibility to investigate aging behavior as a function of rate. Therefore, the current densities were in the range ~ 250 nA/cm up to 750 nA/cm. By monitoring the chamber current, the total collected charge was determined.

Since the average energy losses of α -particles in the chamber cell are much larger than those of X-rays, the same avalanche size as that for X-rays is obtained at a lower voltage. In practice, at an applied voltage of 2.35 kV, the total charge released from α -particles was measured to be a factor of 10-15 larger than that corresponding to a 5.9 keV X-ray localized energy deposition in proportional mode. Moreover, the signals from α 's at this voltage were also accompanied by self-quenching streamer discharges, observed in several percent of the events at this voltage. This may be explained by the fact that since the transformation from proportional to streamer mode depends upon the primary ionization density [74], heavily ionizing particles should enter

the self-quenching streamer mode at lower voltages than Fe^{55} X-rays and minimum ionizing particles.

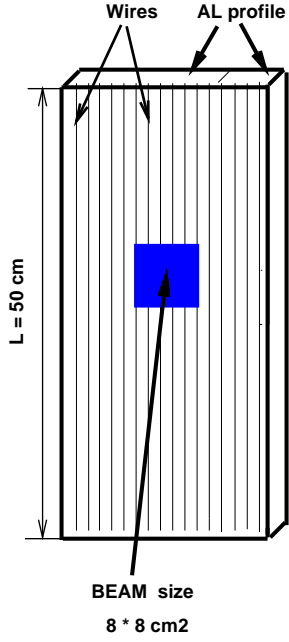


Figure 8: Sketch of the tube chamber used in the α -beam in Karlsruhe.

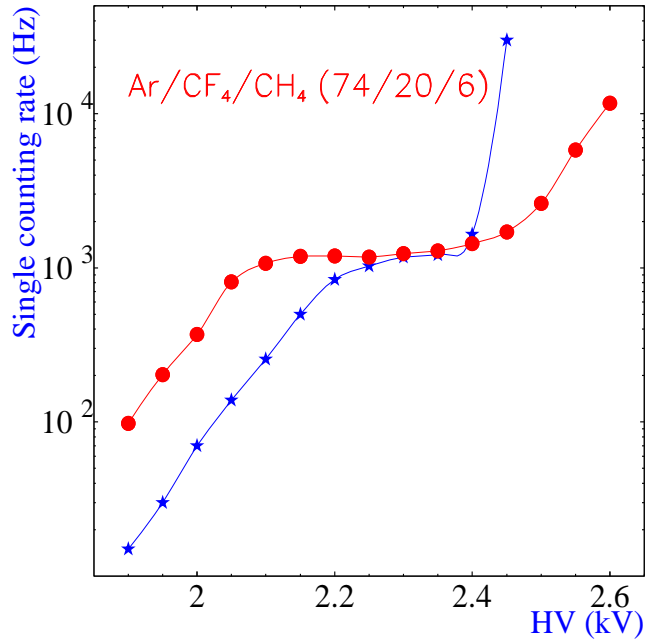


Figure 9: Singles rate curves for the ‘reference wire’ in the irradiated region (stars), after exposure to $60 \frac{mC}{cm \text{ wire}}$, and outside of it (circles).

After the first 24 hours of irradiation, which resulted in a collected charge of $\sim 50 \frac{mC}{cm \text{ wire}}$, the status of the ‘reference wire’ was checked by recording the Fe^{55} pulse-height spectra. Severe anode aging was observed for this wire in the irradiated area, corresponding to a normalized gas gain loss value $R \sim 750 \text{ \% per } C/cm$, while the Fe^{55} spectra in the non-irradiated region remained unchanged. The downward shift of the peak value was accompanied by a distortion and broadening of the Fe^{55} pulse-height spectrum. After the next 6 hours of exposure, when an additional $10 \frac{mC}{cm \text{ wire}}$ were collected, a steady decrease of the gas gain for the ‘reference wire’ has been found, and the R value became even slightly higher $\sim 850 \text{ \% per } C/cm$. Furthermore, during these hours, sizeable increase in the single counting rate, above the actual α -beam intensity, was observed from several of the irradiated wires. Since that time, the irradiation of the ‘reference wire’ was halted, but, the aging studies with all other wires were continued until the collected charge had reached a value of $280 \frac{mC}{cm \text{ wire}}$. Two wires, irradiated over half of their cell width, accumulated half of this charge - $140 \frac{mC}{cm \text{ wire}}$. The aging behavior of the wires during irradiation was quite similar: large increase in the single

counting rate, as a result of spark discharges, was observed from all wires at an applied voltage of 2.35 kV, together with the monotonic drop in the chamber current.

After the aging studies in Karlsruhe, the chamber characteristics have been studied on the 3 GeV electron beam with intensity $\sim 1 \text{ kHz/cm}^2$. Fig. 9 shows the singles rate curves for the ‘reference wire’ in the irradiated region, after exposure to $60 \frac{mC}{cm \text{ wire}}$, and outside of it. From these curves it is seen that, as result of irradiation, there is a shift upwards of the lower end of the efficiency plateau (showing a decrease of gain at a given voltage) with a consequent reduction in effective plateau length. All other irradiated wires were also studied on the electron beam. Wires that have been exposed to a charge of $280 \frac{mC}{cm \text{ wire}}$ were found to be heavily damaged, showing an efficiency at the level of $\sim 1\%-10\%$ for the nominal operating high voltage 2.35 kV. In addition, for all damaged wires the breakdown knee in the singles rate curves significantly displaced towards lower voltages. This effect can also be seen for the ‘reference wire’ in Fig. 9. For the damaged region of this wire, the breakdown point occurs at $\text{HV}=2.45 \text{ kV}$, where the single counting rate increases abruptly. At the same time, whenever the electrons illuminates regions of the wire that have not been previously irradiated, no actual difference in the singles rate curves (before and after irradiation) shows up.

After the beam tests, the chamber was opened for inspection and both anode wires and cathodes surfaces were analyzed, using microscope and later scanning electron microscopy (SEM). Observation of all damaged wires under a microscope show vertically structured black deposits or ‘whiskers’ (see Fig. 12), distributed randomly within the irradiated area only, and of up to lengths of $50 \mu\text{m}$ from the wire surface. The ‘whiskers’ were found to be very fragile, and easily broken if touched. Of special interest, there were two wires at the boundaries of the irradiated area where only half of the cell width was exposed to α ’s. These wires showed significant asymmetries in the ‘whiskers’ (see Fig. 13) with deposits built up on one side of the anode wire towards all of the primary electrons drifted. The observed asymmetries in the anode deposits indicate that even for high ionization densities produced by α -particles, the operating parameters (high voltage, gas mixture) led rather to avalanches well localized on one side of the anode wire rather than to avalanches whose spread was large enough to surround the wire completely.

Examination of all damaged wires by SEM revealed deposits, containing carbon and fluorine as the only detectable elements, thus confirming the pres-

Figure 10: SEM of the 'reference wire' after the accumulated charge of $60 \frac{mC}{cm \text{ wire}}$. C and F elements were identified together with Au signal from the wire material.

Figure 11: SEM of the cathode surface composition in the irradiated region of the wire after exposure to $280 \frac{mC}{cm \text{ wire}}$.

Figure 12: Typical deposits on the anode wire after exposure to $280 \frac{mC}{cm \text{ wire}}$.

Figure 13: Wire irradiated over half of its cell width. Deposits built up on one side of the wire towards all of the primary electrons drifted.

ence of a polymer coating. Moreover, carbon and fluorine signals were also identified in the irradiated regions free of 'whiskers', together with Au signal from the wire material. Fig. 10 shows, as an example, the SEM of the 'reference wire' after the accumulated charge of $60 \frac{mC}{cm \text{ wire}}$. New wires and wires which were exposed to the irradiated gas, but not irradiated themselves, showed peaks only from Au. Unfortunately, this method is unable to detect hydrogen, so hydrocarbons registered as a carbon alone and are also trapped in the polymer coating. SEM analysis of the cathode surface composition in the irradiated region of the wire after exposure to $280 \frac{mC}{cm \text{ wire}}$ was also performed. Translation of peak areas into atomic abundances indicates that the top layer of the cathode consists mainly of *Al*(> 80 %) with some traces of carbon and oxygen (see Fig. 11).

A direct means of investigating the radiation-initiated spark discharges was to separate anode and cathode effects by combining new and aged portions of the tube chamber. When the cathodes of the tubes that had been previously aged were restrung with the new anode wires, the breakdown knee in the singles rate displaced to the higher voltages. Therefore, one reason for the discharges are some local deposits on the anode wires (conductive 'whiskers'). It was reported by Holland [75], that the properties of polymer films can be electrically conductive or insulating according to the carbon to hydrogen ratio and a degree of cross-linking. If a coating is primarily carbon, rather than normal polymers, the conductivity will be much higher. At the same time, the energy and amount of particle bombardment on the surface can very easily change the composition and therefore conductivity. Hydrogen can be easily removed by ion bombardment, so heavy bombardment leads to a more carbonaceous than polymer-like deposit, which may be relevant for the case of irradiation with α -particles.

6 Summary and outlook.

Experimental conditions at HERA-B impose very strong requirements for the gaseous detectors. The high radiation load of the HERA-B experiment results in an accumulated charge of up to $200 \frac{mC}{cm \text{ wire}}$ in the tube chambers. The chamber signals, which are used to form the trigger, must be collected in less than the 96 ns between bunch crossings.

A short description of the criteria which are relevant for the choice of gases in the HERA-B muon detector are discussed and the tube chamber charac-

teristics studied for several Ar/CF_4 -based mixtures are reported. However, the main criteria for the choice of the gases are the aging properties. In this paper, the brief summary of the most recent data focusing on the binary and ternary mixtures, containing Ar , CH_4 , CO_2 and CF_4 is presented. Although, CF_4 gas has been widely used over the last ten years, the results from its usage in the drift tubes are quite controversial. The aging results reported in this paper demonstrate that the aging rate for irradiation with 5.9 keV X -rays and 100 MeV α 's may differ by more than two orders of magnitude. Despite the negligible gas gain loss measured after the long-term irradiation with Fe^{55} X -rays, rapid aging effects observed with α -particles completely ruled out $Ar/CF_4/CH_4$ (74:20:6) mixture as a candidate for operation in the HERA-B high radiation environment, where at least part of the ionization is deposited by heavily ionizing particles. Moreover, from these results it is evident that from the accumulated charge alone, it is not possible to combine the data from the different radiation sources into one consistent model. Therefore, as long as the data from different aging tests can not be combined properly, it is very difficult to give an extrapolation about the lifetime in the real detector. In order to find a link between results in different setups, we also performed aging studies with $Ar/CF_4/CH_4$ (67:30:3) and $Ar/CF_4/CO_2$ (65:30:5) mixtures in the HERA-B environment, under conditions as similar as possible to real ones. In a subsequent paper [44] we will report on the results from these tests, which indicate that the aging rate could also be affected by the mode of operation, size of the irradiated area and water addition.

Acknowledgments.

We express our special appreciation for discussions with Dr. J. Va'vra. We would like to thank Dr. G. Bohm and Wildau Politechnik Institute for the possibility to analyse the wires. We thank to K. Reeves and S. Aplin for reading and correcting this manuscript.

This work was supported by the Deutsches Elektronen-Synchrotron (DESY), by the Alexander von Humboldt-Stiftung and Max Planck Research Award.

References

- [1] T. Lohse *et al.*, HERA-B collaboration, An Experiment to Study CP Violation in the B System Using an Internal Target at the HERA Proton Ring, Proposal, **DESY-PRC 94/04** (1994).
- [2] E. Hartouni *et al.*, HERA-B collaboration, An Experiment to Study CP Violation in the B System Using an Internal Target at the HERA Proton Ring, Design Report, **DESY-PRC 95/01** (1995).
- [3] M. Buchler *et al.*, IEEE Trans. Nucl.Sci., **NS-46** (1999) 126-132.
- [4] T.J. Sumner *et al*, IEEE Trans. Nucl. Sci., **NS-29 (5)** (1982) 1410-1414.
- [5] S.A. Korff and R.D.Present, Phys. Rev. **Vol.65 (9)** (1944) 274-282.
- [6] V. Bawdekar, IEEE Trans. Nucl. Sci **NS-22** (1975) 282-285.
- [7] L. Colli, U. Fracchini, Rev. Sci. Instr. **Vol.23 (1)** (1952) 39-42.
- [8] L.G. Christophorou, Atomic and Molecular Radiation Physics, (Wiley, New York, 1971)
- [9] L.G. Christophorou *et al*, Nucl. Instr. and Meth. **A 163** (1979) 141-149.
- [10] L.G. Christophorou *et al*, Nucl. Instr. and Meth. **A 171** (1980) 491-495.
- [11] J. C. Armitage *et al*, Nucl. Instr. and Meth. **A 271** (1988) 588-496.
- [12] A. Peisert, F. Sauli, CERN 84-08 (1984).
- [13] S. Biagi, Nucl. Instr. and Meth. **A 421** (1999) 234-240.
- [14] M.C. Borgade *et al*, J. Appl. Phys, **Vol.80, (3)** (1996) 1325-1336.
- [15] T.Yamashita *et al*, Nucl. Instr. and Meth. **A 317** (1992) 213-220.
- [16] S.R.Hunter *et al*, J. Appl. Phys, **Vol.58, (8)** (1985) 3001-3015.
- [17] L.G. Christophorou *et al*, Nucl. Instr. and Meth. **A 309** (1991) 160-168.
- [18] L.G. Christophorou (ed.), Electron-Molecule Interactions and Their Applications, vols. 1 and 2, (Academic Press, New York, 1984)
- [19] W.S. Anderson *et al*, Nucl. Instr. and Meth. **A 323** (1992) 273-279.
- [20] L.G. Christophorou *et al*, J. Phys. Chem. Ref. Data, **Vol.25, No.5** (1996) 1341-1388.

- [21] L.G. Piper *et al*, J. Chem. Phys, **Vol.59, (6)** (1973) 3323-3340.
- [22] J.E. Velazco *et al*, J. Chem. Phys, **Vol.69, (10)** (1978) 4357-4373.
- [23] U. Becker *et al*, Nucl. Instr. and Meth. **A 315** (1992) 14-20.
- [24] O. Grimm, Diplomarbeit, University Hamburg, July (1998) (in german)
- [25] M. Beck, Dissertation, University Rostock, June (1999) (in german)
- [26] T.Yamashita *et al*, Nucl. Instr. and Meth. **A 283** (1989) 709-715.
- [27] S. Beingessner, R. Carnegie, Nucl. Instr. and Meth. **A 260** (1987) 210-220.
- [28] G. Charpak *et al*, Nucl. Instr. and Meth. **A 99** (1972) 279-284.
- [29] Proc. Workshop on Radiation Damage to Wire Chambers, Lawrence Berkeley Laboratory (Jan. 1986) LBL-21170.
- [30] J. A. Kadyk, Nucl. Instr. and Meth. **A 300** (1991) 436-479.
- [31] J. Va'vra, ref. [29], pp. 263-294.
- [32] R. Bouclier *et al*, Aging of microstrip gas chambers: problems and solutions, CERN-PPE 96-33 (1996).
- [33] J. Wise *et al*, IEEE Trans. Nucl. Sci **NS-37 (2)** (1990) 470-477.
- [34] J. Wise *et al*, J. Appl. Phys, **Vol.74, (9)** (1993) 5327-5340.
- [35] D. W. Hess, ref. [29], pp. 15-24.
- [36] H. Yasuda, Plasma Polymerization, (Academic Press, 1985)
- [37] L. Malter Phys. Review, **Vol. 50** (1936) 48-58.
- [38] I. Juricic, J. Kadyk, ref. [29], pp. 141-159.
- [39] R. Kotthaus, ref. [29], pp. 161-193.
- [40] R. Openshaw *et al*, IEEE Trans. Nucl. Sci **NS-36 (1)** (1989) 567-571.
- [41] A. Algeri *et al*, Nucl. Instr. and Meth. **A 338** (1994) 348-367.
- [42] V. Pashhoff, Dissertation, University Freiburg, October (1999)

- [43] M. Titov, A Gaseous Muon Detector at the HERA-B experiment, talk given at Nuclear Science Symposium and Medical Imaging Conference, 15-20 October 2000, Lyon, France
- [44] M. Danilov, L. Laptin, I. Tichomirov, M. Titov, Yu. Zaitsev, Aging of gaseous detectors under high-rate irradiation with hadronic particles, in preparation.
- [45] N. Spielberg, D. Tsarnas Rev. Sci. Instr. **Vol.46 (8)** (1975) 1086-1091.
- [46] A. Smith, M. Turner Nucl. Instr. and Meth. **A 192** (1982) 475-481.
- [47] M. Kollefrath *et al*, Nucl. Instr. and Meth. **A 419** (1998) 351-356.
- [48] K. Kwong, Nucl. Instr. and Meth. **A 238** (1985) 265-272.
- [49] V. Paschhoff, M. Spegel, Aging studies for the ATLAS MTD's using $Ar/CO_2(90:10)$, ATLAS muon note-019 (1999).
- [50] I. Boyko *et al*, Aging of aluminum drift tubes filled with $Ar/CO_2/CH_4$ (92:5:3), ATLAS muon note-089 (1995).
- [51] H. Sadrozinski, ref. [29], pp. 121-129.
- [52] C. Mogab *et al*, J. Appl. Phys, **Vol.49, (7)** (1978) 3796-3803.
- [53] M.J. Kushner, J. Appl. Phys, **Vol.53, (4)** (1982) 2923-2938.
- [54] H.F. Winters *et al*, J. Appl. Phys, **Vol.48, (12)** (1977) 4973-4983.
- [55] J. Kadyk *et al*, IEEE Trans. Nucl. Sci **NS-37 (2)** (1990) 478-486.
- [56] R. Openshaw *et al*, Nucl. Instr. and Meth. **A 307** (1991) 298-308.
- [57] G. Alexeev *et al*, Technical design Report for the D0 Forward Muon Tracking Detector Based on Mini-Drift Tubes, D0 Note 3366, (1997)
- [58] B. Baldin *et al*, Technical design of the central muon system, D0 Note 3365, (1997)
- [59] M. Hohlmann, The Outer Tracker of HERA-B, Proceedings of 8th Pisa Meeting on advanced detector, Isola d'Elba'00, Italy (in press)
- [60] H. Kolanoski, Investigation of Aging in the HERA-B Outer Tracker Drift Tubes, talk given at Nuclear Science Symposium and Medical Imaging Conference, 15-20 October 2000, Lyon, France

- [61] T. Akesson *et al*, Nucl. Instr. and Meth. **A 361** (1995) 440-456.
- [62] ATLAS Technical Design Report, CERN (1997)
- [63] A. Romanouk, Choice of materials for the constructio of TRT, ATLAS Internal Note, INDET-98-211 (1998)
- [64] G. Gavrilov *et al*, Aging investigation of ATLAS TRT straws, PNPI-preprint-2328 (1999)
- [65] T. Ferguson *et al*, Possible new mechanism for anode wire aging in gas filled detectors, PNPI-preprint-2331 (1999)
- [66] T. Zeuner, The MSGC-GEM Inner Tracker for HERA-B Nucl. Instr. and Meth. A (Beauty'99 proceedings, in press).
- [67] J. Va'vra *et al*, Nucl. Instr. and Meth. **A 324** (1993) 113-126.
- [68] D.S. Denisov, On using CF_4 as a working gas for drift tubes (in russian), IHEP-preprint-90-16 (1990)
- [69] J. DeWulf *et al*, Nucl. Instr. and Meth. **A 252** (1986) 443-449.
- [70] J.Kadyk *et al*, Nucl. Instr. and Meth. **A 300** (1991) 511-517.
- [71] M. Danilov *et al*, DESY Internal Note 88-090, DESY (1988)
- [72] J. Va'vra, Aging of gaseous detectors, SLAC-PUB-5207 (1990)
- [73] M. Atac, ref. [29], pp. 55-66.
- [74] AN Ji-Gang *et al*, Nucl. Instr. and Meth. **A 267** (1988) 396-407.
- [75] L. Holland, Thin Film Microelectronics (Chapman and Hall Ltd, 1965) p. 157.

This figure "tubeb1.jpg" is available in "jpg" format from:

<http://arxiv.org/ps/hep-ex/0107080v1>

This figure "gr56.jpg" is available in "jpg" format from:

<http://arxiv.org/ps/hep-ex/0107080v1>

This figure "grn88.jpg" is available in "jpg" format from:

<http://arxiv.org/ps/hep-ex/0107080v1>

This figure "test.jpg" is available in "jpg" format from:

<http://arxiv.org/ps/hep-ex/0107080v1>

This figure "wire_irradiated.jpg" is available in "jpg" format from:

<http://arxiv.org/ps/hep-ex/0107080v1>